Mice lacking ANGPTL8 (Betatrophin) manifest disrupted triglyceride metabolism without impaired glucose homeostasis

Yan Wang[a,b,1], Fabiana Quagliarini[b,1], Viktoria Gusarova[c], Jesper Gromada[c], David M. Valenzuela[c], Jonathan C. Cohen[d,2], and Helen H. Hobbs[a,b,d,2]

[a]Howard Hughes Medical Institute and Departments of [b]Molecular Genetics and [d]Internal Medicine, University of Texas Southwestern Medical Center, Dallas, TX 75390; and [c]Regeneron Pharmaceuticals, Tarrytown, NY 10591

Contributed by Helen H. Hobbs, August 16, 2013 (sent for review July 23, 2013)

Angiopoietin-like protein (ANGPTL)8 (alternatively called TD26, RIFL, Lipasin, and Betatrophin) is a newly recognized ANGPTL family member that has been implicated in both triglyceride (TG) and glucose metabolism. Hepatic overexpression of ANGPTL8 causes hypertriglyceridemia and increased insulin secretion. Here we examined the effects of inactivating *Angptl8* on TG and glucose metabolism in mice. *Angptl8* knockout (*Angptl8*$^{-/-}$) mice gained weight more slowly than wild-type littermates due to a selective reduction in adipose tissue accretion. Plasma levels of TGs of the *Angptl8*$^{-/-}$ mice were similar to wild-type animals in the fasted state but paradoxically decreased after refeeding. The lower TG levels were associated with both a reduction in very low density lipoprotein secretion and an increase in lipoprotein lipase (LPL) activity. Despite the increase in LPL activity, the uptake of very low density lipoprotein-TG is markedly reduced in adipose tissue but preserved in hearts of fed *Angptl8*$^{-/-}$ mice. Taken together, these data indicate that ANGPTL8 plays a key role in the metabolic transition between fasting and refeeding; it is required to direct fatty acids to adipose tissue for storage in the fed state. Finally, glucose and insulin tolerance testing revealed no alterations in glucose homeostasis in mice fed either a chow or high fat diet. Thus, although absence of ANGPTL8 profoundly disrupts TG metabolism, we found no evidence that it is required for maintenance of glucose homeostasis.

Adipose tissue is the major energy reservoir in the body and serves to buffer metabolically active tissues against diurnal changes in food intake by releasing free fatty acids into the circulation during fasting. Upon refeeding, adipose tissue is replenished with fatty acids obtained from circulating triglyceride (TG)-rich lipoproteins produced in the gut and liver. Fatty acids are cleaved from lipoprotein TGs by the enzyme lipoprotein lipase (LPL), which is anchored to the capillary endothelial surfaces of peripheral tissues (1). The uptake of TG-fatty acids is controlled by regulating LPL activity in accordance with nutritional status (2). In fasting, LPL activity is reduced in adipose tissue and increased in heart and skeletal muscle, thereby directing TG-fatty acids to muscle for oxidation (3). In the fed state, LPL activity declines in muscle and increases in adipose tissue, directing TG-fatty acids to adipose tissue for storage.

Two angiopoietin-like proteins, ANGPTL3 and ANGPTL4 (4, 5), play roles in the partitioning of TGs in fasting and refeeding. Both ANGPTLs inhibit LPL (6–8). Overexpression of either protein inhibits LPL activity and causes hypertriglyceridemia, whereas loss-of-function mutations lead to very low TG levels (7, 8). ANGPTL4 is expressed at high levels in liver and adipose tissue, primarily in the fasted state (5). It suppresses LPL activity selectively in adipose tissue and redirects TG to muscle (9). ANGPTL3 is expressed almost exclusively in liver and its levels are only modestly altered by fasting and refeeding (10). It has been suggested that ANGPTL3 is involved in the redirection of TGs to adipose tissue during feeding (9), but direct evidence is lacking.

Previously, we showed that ANGPTL8 [also known as TD26, RIFL (11), Lipasin (12), and Betatrophin (13)] acts together with ANGPTL3 (14). ANGPTL8 is expressed at the highest levels in liver and adipose tissue, and is markedly up-regulated by feeding and suppressed by fasting (11, 12, 14). Adenovirus-mediated hepatic overexpression of ANGPTL8 increases plasma TG levels in wild-type mice but not in mice lacking ANGPTL3 (12). Coexpression of ANGPTL8 and ANGPTL3 increased plasma TG levels more than 10-fold, suggesting that the two proteins act together (14). Consistent with this hypothesis, ANGPTL3 and ANGPTL8 can be coimmunoprecipitated in the plasma of mice or in the medium of cells expressing both proteins (14). These data suggest that ANGPTL8 acts together with ANGPTL3 to coordinate the trafficking of TGs to tissues in response to food intake.

Recently, Melton and his colleagues (13) reported that hepatic overexpression of ANGPTL8, which they called Betatrophin, promotes proliferation of pancreatic β-cells and increases insulin secretion. Thus, ANGPTL8 may also contribute to glucose homeostasis. To determine the physiological role of ANGPTL8 in lipid and glucose metabolism, we generated *Angptl8* knockout (*Angptl8*$^{-/-}$) mice and compared their responses to fasting and refeeding with those of their wild-type littermates. Here we show that disruption of *Angptl8* profoundly alters TG metabolism in fed animals. The knockout mice have decreased adipose tissue mass and a pronounced reduction in plasma TG levels in the fed state. Despite an increase in LPL activity, the uptake of very low density lipoprotein (VLDL)-TG into adipose tissue was markedly reduced in fed *Angptl8*$^{-/-}$ mice. These changes in TG metabolism were not associated with significant alterations in glucose homeostasis or insulin levels.

Significance

Here we show that ANGPTL8 plays a major role in the trafficking of triglycerides to peripheral tissues in response to food intake in mice. Circulating triglycerides are predominantly delivered to skeletal muscle and heart during fasting and are partitioned to adipose tissue upon refeeding. The postprandial increase in triglyceride delivery to adipose tissue is abolished in mice lacking ANGPTL8; consequently, the mice fail to replenish triglyceride stores in adipose tissue. Despite major alterations in triglyceride metabolism, no defects in glucose metabolism were detected in *Angptl8*$^{-/-}$ mice. The finding that plasma triglyceride levels are lower in *Angptl8*$^{+/-}$ mice suggests that even partial inhibition of ANGPTL8 may provide therapeutic benefit for treatment of dyslipidemia.

Author contributions: Y.W., F.Q., V.G., J.G., J.C.C., and H.H.H. designed research; Y.W., F.Q., and V.G. performed research; V.G., J.G., and D.M.V. contributed new reagents/analytic tools; Y.W., F.Q., V.G., J.G., J.C.C., and H.H.H. analyzed data; and Y.W., F.Q., J.C.C., and H.H.H. wrote the paper.

The authors declare no conflict of interest.

Freely available online through the PNAS open access option.

[1]Y.W. and F.Q. contributed equally to this work.

[2]To whom correspondence may be addressed. E-mail: jonathan.cohen@utsouthwestern.edu or helen.hobbs@utsouthwestern.edu.

This article contains supporting information online at www.pnas.org/lookup/suppl/doi:10.1073/pnas.1315292110/-/DCSupplemental.

Results

Generation of *Angptl8* Knockout Mice. *Angptl8*$^{-/-}$ mice were generated on a C57BL/6NTac background by homologous recombination (Fig. 1*A*) using VelociGene technology (15). Recombination was confirmed by PCR (Fig. 1*A*) and genomic blotting (Fig. S1*A*). Knockout mice were born in the expected Mendelian ratios and developed normally. Body weights were similar in *Angptl8*$^{-/-}$ and wild-type mice at 12 wk of age, although a small decrease in body fat content and percent body fat was already apparent at that age (Fig. 1*B*). Thereafter, the knockout animals failed to gain weight at the same rate as their wild-type littermates (Fig. 1*C*, *Left*). The difference in body weight was attributable entirely to a reduced accumulation of adipose tissue in the knockout animals (Fig. 1*C*, *Right*). Lean mass was normal in the *Angptl8*$^{-/-}$ mice over this time period (Fig. S1*B*). Metabolic and activity measurements performed over a 5-d monitoring period revealed no differences in oxygen consumption, respiratory exchange ratio, food and water intake, or physical activity between *Angptl8*$^{-/-}$ mice and wild-type littermates (Fig. S2 *A* and *B*). Core body temperatures were similar in the two strains (Fig. S2*C*). Fecal fat excretion was similar in wild-type and knockout animals (17.7 +/– 4.2 vs. 15.5 +/– 1.7 mg/day, p = 0.3)

***Angptl8*$^{-/-}$ Mice Have Reduced Plasma Levels of TG and Nonesterified Fatty Acids.** Mice lacking ANGPTL8 had a 70% reduction in plasma TG levels compared with littermate controls when fed a chow diet ad libitum (Fig. 2*A*). Similar findings were observed previously in *Angptl3*$^{-/-}$ (4, 7), *Angptl4*$^{-/-}$ (7), and *Angptl8*$^{-/-}$ mice that were generated as part of a library of knockout mice with mutations in membrane and secreted proteins (16).

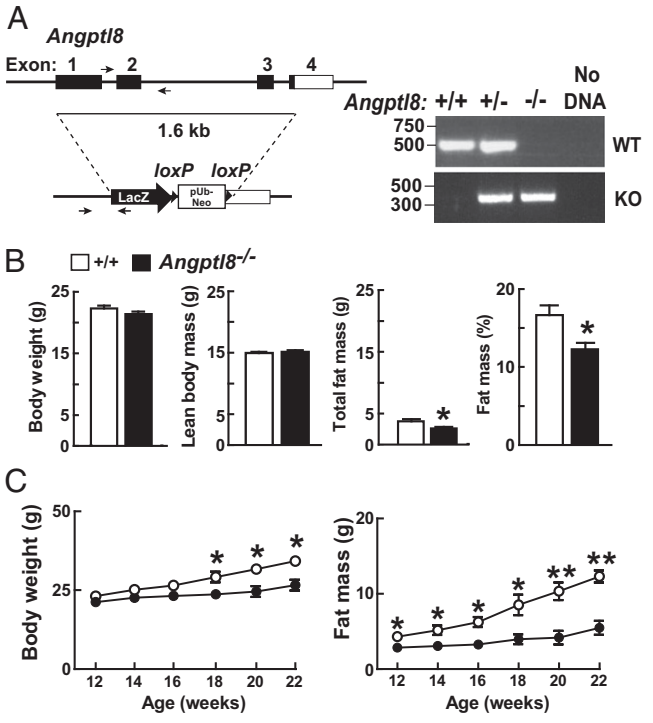

Fig. 1. Development and characterization of *Angptl8* knockout mice. (*A*) Targeted disruption of mouse *Angptl8*. The targeting vector replaced exons 1–3 and part of exon 4 of *Angptl8* (nucleotides 21639965–21641596 of chromosome 9; Genome Build 37, http://www.ncbi.nlm.nih.gov/projects/genome/assembly/grc/mouse/) with a LacZ-pUb-Neo cassette. Genotypes were assayed using PCR and the indicated primers for the wild-type (518 bp) and mutant (357 bp) alleles, as described in *Materials and Methods*. (*B*) Body weight and composition were measured in 10- to 13-wk-old female *Angptl8*$^{-/-}$ mice and wild-type littermates (n = 14–15 per group) as described in *SI Materials and Methods*. (*C*) Body weight and total fat mass were monitored every other week in female *Angptl8*$^{-/-}$ and wild-type mice (n = 4–5 per group, age 12 wk). *P < 0.05, **P < 0.01. Values are means +/– SEM.

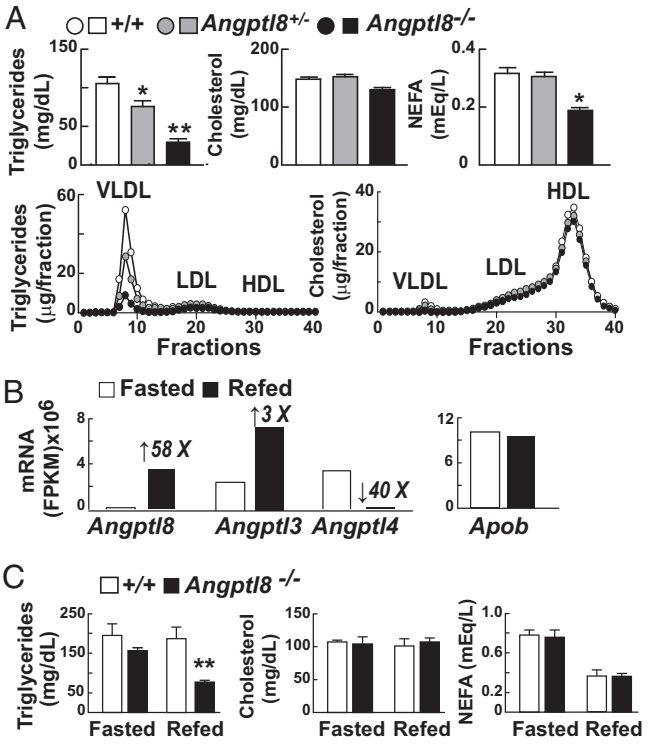

Fig. 2. Effects of *Angptl8* inactivation on lipid metabolism. (*A*) Plasma lipids of male *Angptl8*$^{-/-}$ and *Angptl8*$^{+/-}$ mice and wild-type littermates (n = 4–5 per group, age 10–12 wk) fed a chow diet ad libitum. Samples were collected at 7:00 AM. Pooled plasma from each group was fractionated by FPLC (n = 40 fractions) and the TG and cholesterol contents of each fraction were determined enzymatically. The experiments were repeated three times with similar results. (*B*) Poly(A) mRNA was isolated from livers of three fasted and three refed 10-wk-old male C57BL/6J mice. The mRNA from each group was pooled, reverse-transcribed, and subjected to whole-transcriptome shotgun sequencing (RNA-Seq). Transcript abundance was expressed as fragments per kilobase of exon per million fragments mapped (FPKM). The number above each bar indicates fold change relative to the fasted group. (*C*) *Angptl8*$^{-/-}$ mice and wild-type littermates (n = 4 per group, 8- to 12-wk-old male mice) were habituated for 3 d to a dietary regimen, and plasma lipids were determined in the fasted and fed states as described in *Material and Methods*. *P < 0.05, **P < 0.01. Values are means +/– SEM.

Heterozygotes for the disrupted *Angptl8* allele had plasma TG levels intermediate between those of wild-type and knockout animals, which is consistent with a semidominant pattern of inheritance (Fig. 2*A*). The low plasma TG levels in the *Angptl8*$^{-/-}$ mice reflected a decrease in VLDL-TG content (Fig. 2*A*, *Lower*). No genotype-specific differences in plasma levels of cholesterol were detected in the ANGPTL8-deficient animals (Fig. 2*A*, *Upper*), in contrast to *Angptl3*$^{-/-}$ mice, which have low plasma cholesterol as well as TG levels. Plasma levels of nonesterified fatty acids (NEFAs) were reduced 40% in the *Angptl8*$^{-/-}$ animals fed a chow diet ad libitum (Fig. 2*A*, *Upper*).

Plasma TG Levels Were Reduced in Fed but Not in Fasted *Angptl8*$^{-/-}$ Mice. Previously, we (14) and others (11, 12) showed that expression of ANGPTL8 is increased by food intake. To compare effects of fasting and refeeding on hepatic expression of *Angptl8* with that of *Angptl3* and *Angptl4*, we performed RNA-Seq on hepatic mRNA from wild-type mice. Levels of hepatic *Angptl8* mRNA were extremely low after a 12-h fast, and increased dramatically (58-fold) with refeeding (Fig. 2*B*). In fasted mice, *Angptl3* transcripts were far more abundant than those of *Angptl8*, and the levels increased more modestly with refeeding

(threefold). Expression of *Angptl4* was antiphase to that of *Angptl8* and *Angptl3*, as reported previously (9). Expression of *Apob* is not affected by fasting or refeeding and served as a negative control for this experiment.

Next, we examined the relationship between feeding-induced changes in *Angptl8* expression and plasma lipid levels. After a 12-h fast, when hepatic expression of *Angptl8* was negligible and *Angptl4* was high, plasma TG levels were similar in wild-type and *Angptl8*$^{-/-}$ mice (Fig. 2*C*). Refeeding did not significantly alter plasma TG levels in wild-type mice but dramatically lowered plasma TG in *Angptl8*$^{-/-}$ animals (Fig. 2*C*), reflecting a reduction of TG in the VLDL fraction (Fig. S3).

Fasting and refeeding did not elicit changes in plasma cholesterol levels in the *Angptl8*$^{-/-}$ mice (Fig. 2*C*). The low NEFA levels that were consistently observed in *Angptl8*$^{-/-}$ mice fed ad libitum were not apparent in animals entrained to a 12-h fasting/12-h feeding cycle for 3 d (Fig. 2*C*). The significance of this difference is currently unclear. It is possible that the training period eliminates the difference, or that plasma NEFA levels are only reduced at specific intervals during the fasting/refeeding cycle, and that these intervals do not coincide with the sampling times (7:00 AM and 7:00 PM) in the fasting/refeeding protocol.

Plasma Glucose and Insulin Levels Are Not Altered in Chow-Fed *Angptl8*$^{-/-}$ Mice. Metabolic defects that alter adipose tissue fat accumulation are frequently associated with changes in glucose homeostasis. Plasma glucose and insulin levels in the fasted and fed states did not differ between the *Angptl8*$^{-/-}$ and wild-type mice (Fig. 3*A*). In mice that had been fasted for 12 h, the excursions of blood glucose levels after i.p. administration of a glucose bolus were similar in the *Angptl8*$^{-/-}$ mice and their littermate controls, as were plasma insulin levels measured before and 15 min after glucose administration (Fig. 3*B*). Similar results were obtained in mice fasted for 5 h. Insulin (Fig. 3*C*) and pyruvate (Fig. 3*D*) tolerance tests were performed to assess insulin sensitivity and hepatic gluconeogenesis, respectively. No genotype-specific differences were observed in either the magnitude or the pattern of response of plasma glucose levels to either the insulin or pyruvate bolus. Thus, the changes in plasma TG levels and adipose mass in the *Angptl8*$^{-/-}$ mice were not accompanied by any appreciable changes in blood glucose homeostasis or whole-body insulin sensitivity. Feeding a high-fat diet (60% fat) for 11 wk increased the insulin to glucose ratio (Fig. 3*E*) and impaired glucose tolerance to a similar extent in the wild-type and *Angptl8*$^{-/-}$ mice (Fig. 3*F*).

Reduced VLDL Production Without Hepatic Steatosis in *Angptl8*$^{-/-}$ Mice. To determine whether the reduction in plasma TG levels in the *Angptl8*$^{-/-}$ mice was due to decreased VLDL secretion, we measured the rate of entry of VLDL-TG into plasma after injecting Triton WR-1339 to inhibit intravascular TG hydrolysis (17). As expected, plasma levels of TG before the injection were substantially lower in the *Angptl8*$^{-/-}$ knockout mice (Fig. 4*A*). Following injection of Triton, the rate of increase in plasma TG levels was markedly reduced (6.8 ± 2.3 vs. 13.6 ± 3 mg·dL^{-1}·min^{-1}; $P = 0.007$) in the *Angptl8*$^{-/-}$ mice compared with wild-type littermates. Thus, absence of ANGPTL8 results in a reduction in VLDL secretion.

Primary defects in VLDL secretion, such as those that result from mutations in *Apob* or *Mttp*, are associated with hepatic TG accumulation (18, 19). Hepatic TG levels in fasted and refed *Angptl8*$^{-/-}$ mice were indistinguishable from those of their wild-type littermates (Fig. 4*B*), as were levels of the other major lipids (Fig. S4). This finding suggests that the low rate of VLDL secretion in the *Angptl8*$^{-/-}$ mice is not due to a defect in the machinery required to assemble and secrete VLDL.

To gain further insights into the causes of low VLDL secretion in the *Angptl8*$^{-/-}$ mice, we assayed the levels of key mRNAs involved in hepatic TG metabolism (Fig. S5). No changes were observed in the mRNAs encoding the transcription factors ChREBP and SREBP-1c, which coordinate the expression of genes required for fatty acid synthesis (20, 21), or in the expression of enzymes that catalyze the synthesis of fatty acids. Similarly, we found no changes in expression of PGC-1α or in the enzymes

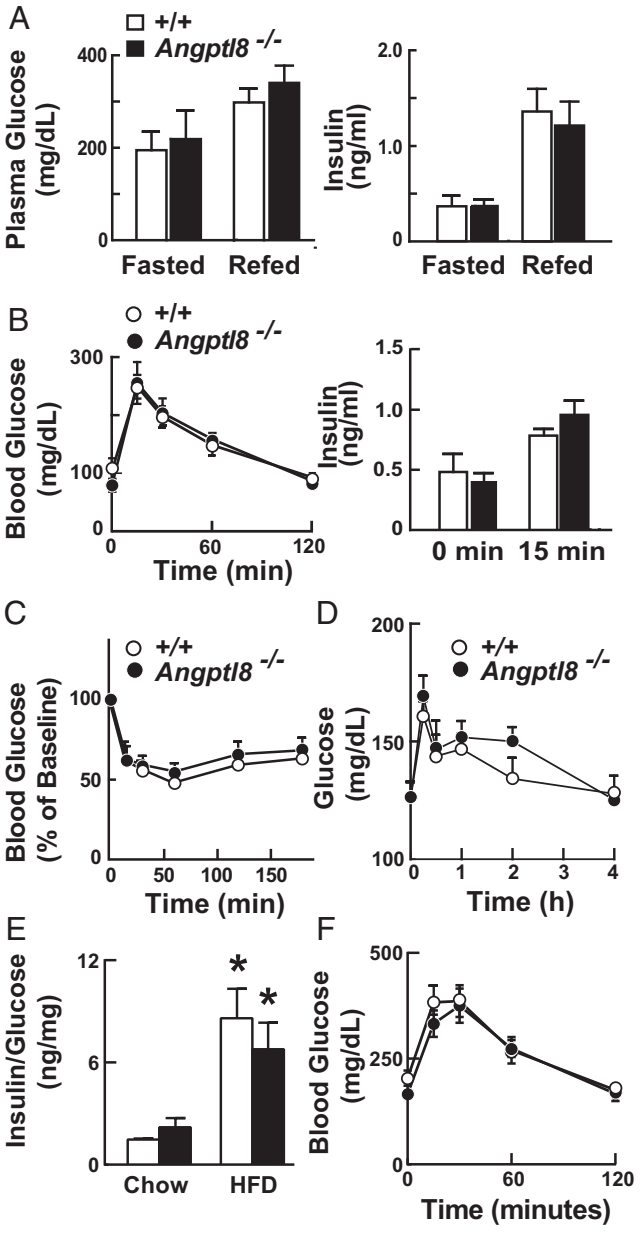

Fig. 3. Glucose homeostasis in *Angptl8*$^{-/-}$ mice. (*A*) Plasma levels of glucose and insulin in fasted and fed *Angptl8*$^{-/-}$ mice. Glucose and insulin concentrations were measured in the same samples as shown in Fig. 2*B* using the Vitros 250 System (GMI) and by ELISA, as described in *Materials and Methods*. (*B*) Glucose tolerance tests performed after overnight fasting in female *Angptl8*$^{-/-}$ mice and wild-type littermates ($n = 5$, age 8–12 wk). Blood glucose and plasma insulin levels were measured using a glucometer and ELISAs as described in *Materials and Methods*. (*C*) Insulin tolerance tests performed after a 4-h fast in female *Angptl8*$^{-/-}$ mice and wild-type littermates ($n = 5$ per group, age 8–12 wk). Blood glucose levels are expressed as percentage of baseline levels. The experiments shown here were repeated with similar results. (*D*) Pyruvate tolerance tests were performed in female *Angptl8*$^{-/-}$ mice and wild-type littermates ($n = 5$ per group, age 12–17 wk) as described in *Materials and Methods*. (*E*) Female *Angptl8*$^{-/-}$ and wild-type littermates ($n = 4$–5 per group, age 10–13 wk) were fed a high-fat diet (HFD; 60% fat) for 11 wk. Plasma glucose and insulin levels were obtained at the end of the dark cycle. *$P < 0.05$. (*F*) Glucose tolerance tests were performed after a 5-h fast and blood glucose levels were measured using a glucometer. This experiment was repeated and the results were similar. Values are means +/− SEM.

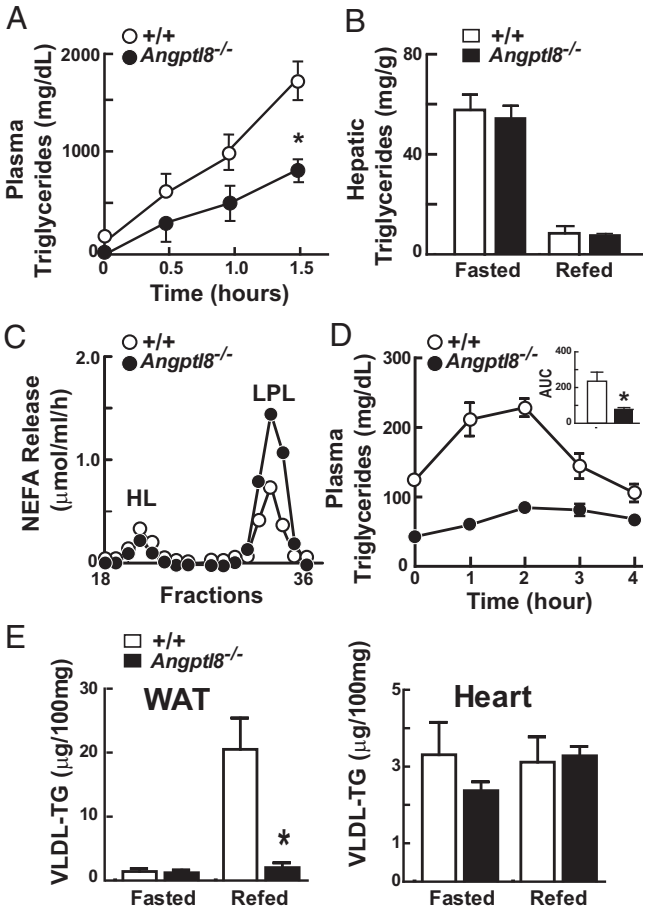

Fig. 4. VLDL secretion and postheparin LPL activity in *Angptl8*$^{-/-}$ mice. (*A*) Plasma TG levels after injection of Triton WR-1339 in chow-fed male *Angptl8*$^{-/-}$ mice and wild-type littermates (n = 4–6 per group, age 20–23 wk). P value for slope = 0.007. (*B*) Hepatic TG levels in *Angptl8*$^{-/-}$ mice and wild-type littermates during fasting and refeeding. The liver samples are from the mice described in Fig. 2*B*. (*C*) Lipase activity in postheparin plasma of *Angptl8*$^{-/-}$ mice and wild-type littermates (n = 6 per group). Postheparin plasma was pooled and fractionated on a heparin column to separate HL and LPL, and TG hydrolase activity was measured as indicated in *SI Materials and Methods*. (*D*) Fat tolerance tests in chow-fed male *Angptl8*$^{-/-}$ mice and wild-type littermates (n = 4–6 per group, age 20–23 wk). The area under the curve (AUC) was calculated by linear interpolation. (*E*) Tissue uptake of VLDL-TG in female *Angptl8*$^{-/-}$ mice during fasting and refeeding (n = 4 per group, age 8 wk). VLDL was labeled with [^{3}H]palmitate as described (36). Mice were entrained for 3 d to a 12-h fasting/12-h refeeding regimen. A total of 120 μg of [^{3}H]VLDL was injected into the circulation of either fasted or refed mice and tissues were collected after 15 min as described in *Materials and Methods*. WAT, white adipose tissue. *P = 0.02. Values are means +/− SEM.

involved in fatty acid oxidation. These data suggest that ANGPTL8 does not alter de novo lipogenesis or fatty acid oxidation at the transcriptional level in the liver, but we cannot exclude the possibility that deficiency of ANGPTL8 elicits posttranscriptional changes in fatty acid biosynthesis or oxidation that decreases the availability of fatty acids for VLDL-TG synthesis.

ANGPTL8 Deficiency Is Associated with a Selective Increase in Postheparin Plasma LPL Activity. ANGPTL8 shares a sequence motif in the N-terminal domain that mediates inhibition of LPL by ANGPTL3 and ANGPTL4 (22). Accordingly, we measured the activity of the two major endothelial TG lipases, hepatic lipase (HL) and LPL, in postheparin plasma from *Angptl8*$^{-/-}$ and wild-type mice. These tests were performed in fed animals because differences in plasma TG levels were not apparent in fasted *Angptl8*$^{-/-}$ mice. Plasma samples from chow-fed knockout and wild-type mice were collected before and 15 min after an i.v. bolus of heparin, which releases LPL from vascular endothelial surfaces. Postheparin plasma was fractionated to separate HL from LPL (1). A selective increase in LPL activity was found in *Angptl8*$^{-/-}$ mice (Fig. 4*C*). We confirmed these results by measuring total lipase activity in preheparin and postheparin plasma. Preheparin lipase activity, which is predominantly due to the action of HL (23), was not increased, whereas postheparin lipase activity, which includes both HL and LPL, was increased in the *Angptl8*$^{-/-}$ mice (Fig. S6*A*). LPL activity, which was estimated by subtracting preheparin from postheparin lipase activity, was increased (Fig. S6*A*). Thus, LPL activity was found to be selectively increased in *Angptl8*$^{-/-}$ mice using two different methods of measurement. Real-time PCR of adipose tissue, skeletal muscle, heart, and brown adipose tissue revealed no significant differences in LPL mRNA levels between the two strains (Fig. S6*B*). Therefore, the increased postheparin plasma LPL activity in *Angptl8*$^{-/-}$ mice did not reflect increased LPL mRNA levels in the major sites of LPL expression.

Accelerated Clearance of Dietary Fat in *Angptl8*$^{-/-}$ Mice. The increased heparin-releasable LPL activity observed in the *Angptl8*$^{-/-}$ mice would be predicted to accelerate clearance of circulating TG-rich lipoproteins. To assess TG clearance in these animals, we performed oral fat tolerance tests. The excursion of plasma TG levels following an oil gavage was markedly attenuated in *Angptl8*$^{-/-}$ mice (Fig. 4*D*), consistent with increased LPL-mediated hydrolysis of circulating TG. Because VLDL and chylomicrons compete for LPL, we cannot exclude the possibility that the decreased postprandial TG excursion in *Angptl8*$^{-/-}$ mice reflects decreased competition from VLDL-TG. Nonetheless, the increased postheparin plasma LPL activity and decreased postprandial lipemia in the *Angptl8*$^{-/-}$ mice suggest that clearance of circulating TG-rich lipoproteins is accelerated in these animals.

ANGPTL8 Is Required for Increased Postprandial Uptake of VLDL-TG by Adipose Tissue. To determine the effect of ANGPTL8 deficiency on the trafficking of TG to peripheral tissues, we measured tissue uptake of VLDL-[^{3}H]palmitate. Labeled VLDL was generated by infusing wild-type mice with [^{3}H]palmitate complexed with albumin, isolated by ultracentrifugation, and then infused into *Angptl8*$^{-/-}$ mice and their wild-type littermates. In wild-type mice, uptake of VLDL-TGs into adipose tissue was very low in the fasted state and increased dramatically with refeeding (Fig. 4*E*). In contrast, the feeding-induced increase in VLDL-TG uptake by adipose tissue was abolished in the knockout animals. No significant differences in VLDL-TG uptake into heart were seen between wild-type and *Angptl8*$^{-/-}$ in either fasted or fed mice.

ANGPTL8 Is Not Required for Cleavage of ANGPTL3. ANGPTL3 is cleaved to yield an N-terminal domain that contains the LPL binding site and a C-terminal fibrinogen-like domain (24). Coexpression of ANGPTL8 and ANGPTL3 in cultured cells increased the appearance of the N-terminal domain of ANGPTL3 in the medium, suggesting that ANGPTL8 activates ANGPTL3 by promoting its cleavage (14).

Based on these results, we predicted that the *Angptl8*$^{-/-}$ mice would have an increase in full-length ANGPTL3 and a reduction in circulating levels of the N-terminal fragment. Immunoblot analysis of plasma revealed an increase in full-length ANGPTL3 in *Angptl8*$^{-/-}$ mice, as anticipated (Fig. 5), but in contrast to our expectations the levels of the N-terminal fragment were also increased in the plasma of the *Angptl8*$^{-/-}$ mice. These data demonstrate that ANGPTL8 is not essential for cleavage of ANGPTL3.

Discussion

The findings reported in this paper implicate ANGPTL8 as a key mediator of the postprandial trafficking of TG-fatty acids to adipose tissue. Inactivation of *Angptl8* disrupted the metabolism of circulating TGs and resulted in a selective reduction in

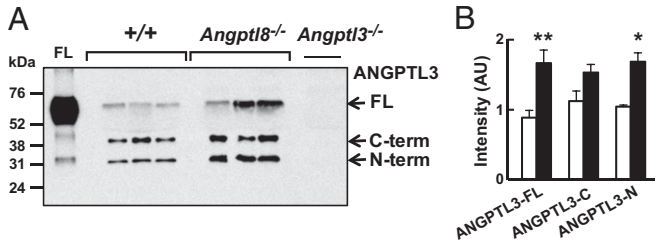

Fig. 5. Immunoblot (*A*) and quantification (*B*) of ANGPTL3 in nonreduced serum from fed mice of the indicated genotypes using a polyclonal anti-mouse ANGPTL3 antibody. Films were scanned using an HP Scanjet 5590 and quantified using ImageJ (National Institutes of Health). The intensity of each band was corrected for background using a blank from the same film. $*P < 0.05$, $**P < 0.01$. The experiments shown here were repeated with similar results. FL, full-length. Values are means +/− SEM.

adipose tissue mass that worsened with age. The metabolic effects of ANGPTL8 deficiency were apparent in the postprandial state. Plasma levels of TG in *Angptl8*$^{-/-}$ mice were comparable to those of wild-type in the fasted state, but were reduced >50% in fed animals. The decrease in plasma TGs reflected major alterations in both production and clearance of circulating TG: secretion of VLDL was markedly reduced and intravascular LPL activity and chylomicron-TG clearance were significantly increased in the knockout animals. Direct measurement of VLDL-fatty acid uptake by adipose tissue and heart revealed substantial differences between wild-type and knockout mice in the fed state. The striking postprandial increase in VLDL-fatty acid uptake into adipose tissue observed in wild-type mice was abolished in the *Angptl8*$^{-/-}$ animals. Taken together, these data reveal that ANGPTL8 plays a major role in replenishing adipose tissue TG stores after fasting.

The transition from fasting to refeeding includes two major changes in the partitioning of energy substrates: the conversion of excess dietary carbohydrates to fatty acids, and the rerouting of TG-fatty acids from oxidative tissues to adipose tissue. Although both of these processes are controlled by insulin, the intermediary regulatory mechanisms appear to be separate. The conversion of carbohydrates to fatty acids is orchestrated by the transcription factors sterol regulatory element binding protein 1 (SREBP1c) and carbohydrate response element binding protein (ChREBP), which promote the transcription of enzymes required for de novo lipogenesis in response to insulin (21, 25). Genetic disruption of the SREBP pathway markedly reduces fatty acid synthesis in liver (26), but does not prevent up-regulation of ANGPTL8 with refeeding (14). It remains possible that ANGPTL8 is a ChREBP target gene. Alternatively, it may be regulated by a heretofore uncharacterized transcriptional pathway.

The impaired VLDL synthesis and increased LPL activity in postprandial plasma of *Angptl8*$^{-/-}$ mice suggest that ANGPTL8 promotes trafficking of TG to adipose tissue by increasing the secretion of hepatic VLDL and inhibiting LPL activity in oxidative tissues. The specific mechanisms by which ANGPTL8 effects these changes remain to be fully defined. In wild-type animals, VLDL secretion is largely substrate-driven (27). Whereas the decrease in circulating NEFA concentrations observed in ad libitum-fed *Angptl8*$^{-/-}$ mice may indicate a reduced availability of fatty acids for hepatic TG synthesis, the absence of any reduction in liver TG content in these animals suggests this is not the case. Definitive answers to the riddle of VLDL underproduction in the *Angptl8*$^{-/-}$ mice will require direct studies of hepatic fatty acid and TG synthesis as well as β-oxidation.

In wild-type rodents, feeding reduces LPL activity in heart and skeletal muscle and increases activity of the enzyme in adipose tissue (3). The high postheparin plasma LPL activity in fed *Angptl8*$^{-/-}$ mice presumably reflects a failure to suppress the enzyme in heart and skeletal muscle, which constitute the major sites of LPL activity. VLDL-TG uptake into heart was preserved in *Angptl8*$^{-/-}$ mice despite a 50% reduction in circulating TG levels, consistent with the maintenance of high LPL activity in this organ. Continued uptake of TG by oxidative tissues, as occurs in transgenic mice that overexpress LPL in skeletal muscle (28), limits the availability of TG for uptake by adipose tissue. The sustained activity of LPL in oxidative tissues compounds the effect of decreased hepatic VLDL-TG secretion, and may abrogate the postprandial increase in VLDL-TG uptake by adipose tissue in *Angptl8*$^{-/-}$ mice. Consequently, adipose tissue is not adequately replenished after fasting in these animals and they fail to accumulate fat as they age.

Because the postprandial increase in adipose tissue LPL activity occurs in the context of increasing ANGPTL8 expression, it is possible that ANGPTL8 spares LPL in this organ. Garcia-Arcos et al. (29) showed that inactivation of LPL in white adipose tissue did not significantly reduce adipose tissue mass in mice unless the mice concurrently overexpressed LPL in muscle. Whereas ANGPTL8 may have differential effects on LPL activity in muscle and adipose tissue, these data suggest that suppression of LPL in oxidative tissues is essential to the accretion of fat in chow-fed animals.

Our data support a model in which ANGPTL8, together with ANGPTL3 and ANGPTL4, coordinates the trafficking of TG and fatty acids in response to diurnal variation in food intake. The three proteins share functional motifs and act on the same metabolic pathways, but in opposing directions and at different phases of the metabolic cycle. Whereas the antiphase expression and metabolic roles of these three ANGPTLs are well-supported, the nature of their interactions has not been fully defined. We (30) and others (31) showed previously that ANGPTL4 functions as a homooligomer. We found no evidence for interaction between ANGPTL4 and ANGPTL3. In contrast, several lines of evidence indicate that ANGPTL8 and ANGPTL3 form a functional complex (14). The low plasma TG levels and high LPL activity in *Angptl8*$^{-/-}$ mice strongly resemble the phenotype of mice lacking ANGPTL3 (7) and further support the notion that the two proteins act in concert.

Some apparent differences between *Angptl3*$^{-/-}$ and *Angptl8*$^{-/-}$ mice may be due to differences in experimental conditions. Shimizugawa et al. reported that VLDL secretion was normal in *Angptl3*$^{-/-}$ mice (8). However, those studies were performed in fasted animals, when the effects of ANGPTL8 would be least apparent, whereas our studies were performed at the end of the dark cycle in food-replete animals. If ANGPTL3 and ANGPTL8 work in concert, as our previous studies suggest (14), then *Angptl3*$^{-/-}$ mice may also manifest reduced VLDL production in the fed state.

Melton and his colleagues implicated ANGPTL8 in pancreatic β-cell proliferation (13). In that study, transient overexpression of ANGPTL8 in the liver increased β-cell mass and insulin secretion (13). The absence of any defect in glucose or insulin tolerance in the *Angptl8*$^{-/-}$ mice indicates that ANGPTL8 is not required for the normal development and function of pancreatic β-cells or for the maintenance of glucose tolerance in chow-fed or fat-fed mice. Our data do not exclude the possibility that ANGPTL8 plays a role in other insulin-resistant states. Alternatively, supraphysiological concentrations of ANGPTL8 may induce b-cell proliferation, but this would be expected to cause hypertriglyceridemia. Other family members, including ANGPTL3, have been shown to promote proliferation of hematopoietic stem cells (32–34).

Human homozygotes for loss-of-function mutations in *ANGPTL3* have markedly reduced plasma levels of both cholesterol and triglyceride (35). Genetic deficiency of ANGPTL8 has not yet been described in humans, but common genetic variation in ANGPTL8 is associated with modest changes in plasma lipid levels (14). Nonetheless, low plasma TG levels and the reduction in adipose tissue with preserved lean mass in the *Angptl8*$^{-/-}$ mice make ANGPTL8 a potentially attractive therapeutic target for dyslipidemia and possibly obesity. The finding that TG levels are lower in *Angptl8*$^{+/-}$ heterozygotes suggests that even partial inhibition of ANGPTL8 may provide therapeutic benefit.

Materials and Methods

Mice. *Angptl8*$^{-/-}$ mice were generated in C57BL/6NTac mice (Taconic) by homologous recombination using VelociGene technology (VG18577) as

previously described (15). Mice were housed (two to four per cage) in a controlled environment (12-h light/12-h dark daily cycle, 23 ± 1 °C, 60–70% humidity), and fed ad libitum with standard chow (Harlan; Teklad 2016). Some mice were fed a high-fat diet (Harlan; Teklad TD06414; 60% fat by calories). For all experiments reported in this paper, comparisons were made between wild-type and knockout littermates. All research protocols involving mice were reviewed and approved by the Institutional Animal Care and Use Committee (University of Texas Southwestern Medical Center and Regeneron Pharmaceuticals).

For fasting and refeeding experiments, mice were trained for 3 d by removing food during the day (7:00 AM to 7:00 PM) and providing food only at night (7 PM to 7:00 AM). Mice were then either fasted for 12 h during the dark cycle (fasted group) or refed for 12 h during the dark cycle after a 12-h fast (refed group). Both groups were killed at 7:00 AM.

Blood and Tissue Chemistries. Plasma and tissue lipids were measured using commercial reagents as described in *SI Materials and Methods*.

Glucose, Insulin, Pyruvate, and Fat Tolerance Testing. For glucose tolerance test, mice were fasted (5 or 16 h) and then given glucose (1.5 g/kg in chow-fed mice, 2 g/kg lean body mass in fat-fed mice) by i.p. injection. Blood samples were obtained from the tail vein at the indicated times and glucose levels were measured using a glucometer (Contour; Bayer). Before and 15 min after glucose injection, 20 μL of blood was collected and plasma was isolated for insulin assays. Insulin levels were measured by ELISA (Ultra Sensitive Mouse Insulin ELISA Kit; Crystal Chem) according to the instructions of the manufacturer.

Insulin tolerance tests were performed in mice fasted for 4 h (7:00 AM to 11:00 AM). Human insulin (Novolin; Eli Lilly; 0.75 unit/kg) was injected into the peritoneal cavity, and blood glucose levels were measured by glucometer (Contour; Bayer) at the indicated times.

Fat tolerance tests were performed at 7:00 AM in mice maintained on ad libitum chow diets. Mice were gavaged with 200 μL corn oil/20 g body weight and blood samples were collected at the indicated times. Plasma TG levels were determined using a colorimetric assay (Infinity; Thermo Scientific).

Pyruvate tolerance tests were performed at 7:00 AM in mice maintained on ad libitum chow diets. A total of 2 mg/kg of pyruvate was injected into the peritoneal cavity and blood glucose levels were measured by glucometer (Contour; Bayer) at the indicated times.

VLDL Secretion. Mice were injected with a bolus of 500 mg/kg Triton WR-1339 (Tyloxapol; Sigma-Aldrich) via the tail vein. Blood was collected from the tail vein at the indicated time points and assayed for plasma levels of TG using a colorimetric assay (Infinity; Thermo Scientific).

Lipase Assays. The activities of lipoprotein lipase and hepatic lipase were assayed in pre- and postheparin plasma (*SI Materials and Methods*).

Preparation of radiolabeled VLDL. VLDL labeling was performed as described (ref. 36 and *SI Materials and Methods*).

VLDL-TG uptake into tissues of* Angptl8$^{-/-}$ *mice. *Angptl8*$^{-/-}$ and wild-type mice were entrained for 3 d to a regimen of 12-h fasting (7:00 AM to 7:00 PM) and 12-h feeding (7:00 PM to 7:00 AM). On day 4, VLDL-TG uptake experiments were performed at 7:00 PM (fasted) or 7:00 AM (fed). Each mouse was injected with 120 μg of ^{3}H-labeled VLDL (1,300 dpm/μg) via the tail vein. After 15 min, mice were anesthetized with isoflurane and perfused with 10 mL of saline via the left ventricle. Tissues were collected immediately after the perfusion and 50-mg pieces were solubilized with 1 mL of SOLVABLE (PerkinElmer) solution and counted. Plasma specific activity was determined from the counts in the injected dose divided by the plasma TG concentration. Total tissue TG uptake was calculated by multiplying tissue counts by the plasma specific activity.

Immunoblotting. Immunoblot analysis was performed exactly as described previously (ref. 14 and *SI Materials and Methods*).

Statistics. Data are expressed as means ± SDs. Mean values were compared using unpaired *t* tests as implemented in Prism (GraphPad Software).

ACKNOWLEDGMENTS. We acknowledge Guosheng Liang, Joe Goldstein, Mike Brown, and Jay Horton for helpful discussions and Christina Zhao and Shahid Tannu for technical assistance. This work was supported by a grant from the National Institutes of Health (RL1HL092550).

1. Beigneux AP, et al. (2007) Glycosylphosphatidylinositol-anchored high-density lipoprotein-binding protein 1 plays a critical role in the lipolytic processing of chylomicrons. *Cell Metab* 5(4):279–291.
2. Wang H, Eckel RH (2009) Lipoprotein lipase: From gene to obesity. *Am J Physiol Endocrinol Metab* 297(2):E271–E288.
3. Kuwajima M, Foster DW, McGarry JD (1988) Regulation of lipoprotein lipase in different rat tissues. *Metabolism* 37(6):597–601.
4. Koishi R, et al. (2002) Angptl3 regulates lipid metabolism in mice. *Nat Genet* 30(2):151–157.
5. Kersten S, et al. (2000) Characterization of the fasting-induced adipose factor FIAF, a novel peroxisome proliferator-activated receptor target gene. *J Biol Chem* 275(37):28488–28493.
6. Yoshida K, Shimizugawa T, Ono M, Furukawa H (2002) Angiopoietin-like protein 4 is a potent hyperlipidemia-inducing factor in mice and inhibitor of lipoprotein lipase. *J Lipid Res* 43(11):1770–1772.
7. Köster A, et al. (2005) Transgenic angiopoietin-like (angptl)4 overexpression and targeted disruption of angptl4 and angptl3: Regulation of triglyceride metabolism. *Endocrinology* 146(11):4943–4950.
8. Shimizugawa T, et al. (2002) ANGPTL3 decreases very low density lipoprotein triglyceride clearance by inhibition of lipoprotein lipase. *J Biol Chem* 277(37):33742–33748.
9. Mattijssen F, Kersten S (2012) Regulation of triglyceride metabolism by Angiopoietin-like proteins. *Biochim Biophys Acta* 1821(5):782–789.
10. Ge H, et al. (2005) Differential regulation and properties of angiopoietin-like proteins 3 and 4. *J Lipid Res* 46(7):1484–1490.
11. Ren G, Kim JY, Smas CM (2012) Identification of RIFL, a novel adipocyte-enriched insulin target gene with a role in lipid metabolism. *Am J Physiol Endocrinol Metab* 303(3):E334–E351.
12. Zhang R (2012) Lipasin, a novel nutritionally-regulated liver-enriched factor that regulates serum triglyceride levels. *Biochem Biophys Res Commun* 424(4):786–792.
13. Yi P, Park JS, Melton DA (2013) Betatrophin: A hormone that controls pancreatic β cell proliferation. *Cell* 153(4):747–758.
14. Quagliarini F, et al. (2012) Atypical angiopoietin-like protein that regulates ANGPTL3. *Proc Natl Acad Sci USA* 109(48):19751–19756.
15. Valenzuela DM, et al. (2003) High-throughput engineering of the mouse genome coupled with high-resolution expression analysis. *Nat Biotechnol* 21(6):652–659.
16. Tang T, et al. (2010) A mouse knockout library for secreted and transmembrane proteins. *Nat Biotechnol* 28(7):749–755.
17. Millar JS, Cromley DA, McCoy MG, Rader DJ, Billheimer JT (2005) Determining hepatic triglyceride production in mice: Comparison of poloxamer 407 with Triton WR-1339. *J Lipid Res* 46(9):2023–2028.
18. Lin X, Schonfeld G, Yue P, Chen Z (2002) Hepatic fatty acid synthesis is suppressed in mice with fatty livers due to targeted apolipoprotein B38.9 mutation. *Arterioscler Thromb Vasc Biol* 22(3):476–482.
19. Raabe M, et al. (1999) Analysis of the role of microsomal triglyceride transfer protein in the liver of tissue-specific knockout mice. *J Clin Invest* 103(9):1287–1298.
20. Uyeda K, Repa JJ (2006) Carbohydrate response element binding protein, ChREBP, a transcription factor coupling hepatic glucose utilization and lipid synthesis. *Cell Metab* 4(2):107–110.
21. Horton JD, Goldstein JL, Brown MS (2002) SREBPs: Activators of the complete program of cholesterol and fatty acid synthesis in the liver. *J Clin Invest* 109(9):1125–1131.
22. Lee EC, et al. (2009) Identification of a new functional domain in angiopoietin-like 3 (ANGPTL3) and angiopoietin-like 4 (ANGPTL4) involved in binding and inhibition of lipoprotein lipase (LPL). *J Biol Chem* 284(20):13735–13745.
23. Dallinga-Thie GM, et al. (2007) Appraisal of hepatic lipase and lipoprotein lipase activities in mice. *J Lipid Res* 48(12):2788–2791.
24. Ono M, et al. (2003) Protein region important for regulation of lipid metabolism in angiopoietin-like 3 (ANGPTL3): ANGPTL3 is cleaved and activated in vivo. *J Biol Chem* 278(43):41804–41809.
25. Iizuka K, Bruick RK, Liang G, Horton JD, Uyeda K (2004) Deficiency of carbohydrate response element-binding protein (ChREBP) reduces lipogenesis as well as glycolysis. *Proc Natl Acad Sci USA* 101(19):7281–7286.
26. Kuriyama H, et al. (2005) Compensatory increase in fatty acid synthesis in adipose tissue of mice with conditional deficiency of SCAP in liver. *Cell Metab* 1(1):41–51.
27. Lewis GF (1997) Fatty acid regulation of very low density lipoprotein production. *Curr Opin Lipidol* 8(3):146–153.
28. Jensen DR, et al. (1997) Prevention of diet-induced obesity in transgenic mice overexpressing skeletal muscle lipoprotein lipase. *Am J Physiol* 273(2 Pt 2):R683–R689.
29. Garcia-Arcos I, et al. (2013) Adipose-specific lipoprotein lipase deficiency more profoundly affects brown than white fat biology. *J Biol Chem* 288(20):14046–14058.
30. Yin W, et al. (2009) Genetic variation in ANGPTL4 provides insights into protein processing and function. *J Biol Chem* 284(19):13213–13222.
31. Ge H, et al. (2004) Oligomerization and regulated proteolytic processing of angiopoietin-like protein 4. *J Biol Chem* 279(3):2038–2045.
32. Zhang CC, et al. (2006) Angiopoietin-like proteins stimulate ex vivo expansion of hematopoietic stem cells. *Nat Med* 12(2):240–245.
33. Khoury M, et al. (2011) Mesenchymal stem cells secreting angiopoietin-like-5 support efficient expansion of human hematopoietic stem cells without compromising their repopulating potential. *Stem Cells Dev* 20(8):1371–1381.
34. Zheng J, et al. (2011) Ex vivo expanded hematopoietic stem cells overcome the MHC barrier in allogeneic transplantation. *Cell Stem Cell* 9(2):119–130.
35. Musunuru K, et al. (2010) Exome sequencing, ANGPTL3 mutations, and familial combined hypolipidemia. *N Engl J Med* 363(23):2220–2227.
36. Aalto-Setälä K, et al. (1992) Mechanism of hypertriglyceridemia in human apolipoprotein (apo) CIII transgenic mice. Diminished very low density lipoprotein fractional catabolic rate associated with increased apo CIII and reduced apo E on the particles. *J Clin Invest* 90(5):1889–1900.